



Rapid identification of ophiopogonins and ophiopogonones in *Ophiopogon japonicus* extract with a practical technique of mass defect filtering based on high resolution mass spectrometry

Tong Xie¹, Yan Liang¹, Haiping Hao^{*}, Jiye A, Lin Xie, Ping Gong, Chen Dai, Linsheng Liu, An Kang, Xiao Zheng, Guangji Wang^{**}

State Key Laboratory of Natural Medicines, Key Lab of Drug Metabolism & Pharmacokinetics, China Pharmaceutical University, Tongjiaxiang 24, Nanjing 210009, China

ARTICLE INFO

Article history:

Received 6 October 2011

Received in revised form 5 January 2012

Accepted 6 January 2012

Available online 14 January 2012

Keywords:

LCMS-Q-TOF

Mass defect filtering

LCMS-IT-TOF

Ophiopogonin

Ophiopogonone

ABSTRACT

This study was to develop and evaluate a practical approach of mass defect filtering (MDF), a post-acquisition data processing technique, for the rapid classification of complicated peaks into well-known chemical families based on the exact mass acquired by high resolution mass spectrometry. The full-scan LC-MS/MS data of the *Ophiopogon japonicus* extract was acquired using high performance liquid chromatography coupled with hybrid quadrupole-time of flight (LCMS-Q-TOF) system which features high resolution, mass accuracy, and sensitivity. To remove the interferences of the complex matrix, MDF approach was developed and employed to rapidly pick out the peaks of ophiopogonins and ophiopogonones from full-scan mass chromatograms. The accuracy of MDF was evaluated in reference to the result of structural identification. After the MDF based classification, both target and non-target components in *Ophiopogon japonicus* extract were characterized based on the detailed fragment ions analysis in the hybrid ion trap and time-of-flight mass spectrometry (LCMS-IT-TOF). By this approach, more than 50 ophiopogonins and 27 ophiopogonones were structurally characterized. The present results of rapid detection and identification of ophiopogonins and ophiopogonones suggest that the proposed MDF approach based on the high-resolution mass spectrometry data would be expected adaptable to the analysis of other herbal components.

© 2012 Elsevier B.V. All rights reserved.

1. Introduction

With significant expansion of the use of Traditional Chinese Medicines (TCMs) based on their long clinical practice, more efforts should be devoted to develop effective and reliable methodologies with the capability of comprehensive structural characterization to guarantee their identity, consistency, and authenticity in the process of “modernization” and “globalization” [1–3]. *Ophiopogon japonicus* is a popular TCM for the treatment and prevention of cardiovascular diseases. On the basis of previous researches, ophiopogonin and ophiopogonone have been reported as the active components in *Ophiopogon japonicus* [4,5]. However, no research was currently available concerned with a methodology for comprehensive identification of such active components in *Ophiopogon japonicus*.

^{*} Corresponding author. Tel.: +86 2583271179; fax: +86 2583271060.

^{**} Corresponding author. Tel.: +86 2583271128; fax: +86 2583302827.

E-mail addresses: hph.770505@yahoo.com.cn (H. Hao),

guangjiwang@hotmail.com (G. Wang).

¹ These two authors contributed equally to this work.

Currently, a large-scale performance of analysis relies heavily on the continuous innovation of analytical techniques, like liquid chromatography–mass spectrometry (LC-MS), gas chromatography–mass spectrometry (GC-MS), capillary electrophoresis–mass spectrometry (CE-MS), liquid chromatography–nuclear magnetic resonance (LC-NMR), and combination of chemical and biological methods [6–8]. LC-MS exhibits an excellent performance to analyze multi-components in complex matrices due to its specificity and sensitivity. In this regard, the AB SCIEX TripleTOF™ mass spectrometry is a high-resolution hybrid quadrupole time-of-flight mass spectrometer (Q-TOF-MS) for qualitative analysis that has the resolution of 25,000 FWHM at low mass (m/z 100) and up to 40,000 at m/z 950, at 100 spectra/s [9]. Besides, it features the highest detection sensitivity, high-speed with stable ~1 ppm mass accuracy over days of acquisition and an acquisition speed up to 100 spectra per second. In this study, a liquid chromatography coupled with full scan high resolution mass spectrometry (LC-HRMS) method for detection of ophiopogonins and ophiopogonones in *Ophiopogon japonicus* extract based on LCMS-Q-TOF (AB SCIEX TripleTOF™ system) was developed.

In previous reports, the detection of the TCM components from the full-scan mass chromatograms using LCMS-TOF was usually

performed manually one by one [10,11]. Obviously, manual inspection was low-effective and labor-intensive. Moreover, it was often difficult and error-prone to distinguish the relatively small signals from the complex chemical background in full-scan mass chromatograms. Although numerous literatures had put great emphasis on the detection and identification of complex components in herbal extracts based on MS/MS or MSⁿ fragmentation [12,13], very few research could provide an automatic and high throughput method. We have recently described a “diagnostic fragment-ion-based extension” strategy to rapidly screen and identify the serial components in *Shenmai* injection, which undoubtedly improved analytical efficiency [14]; however, this approach was largely dependent on predefined fragments summarized from standards. Mass defect filtering (MDF), a data processing technique integrated in the Peakview software (developed by AB SCIEX cooperation), presented a novel approach to tackling the problem. Initially, MDF technique was developed for metabolites detection purposes based on a narrow and well-defined mass defect range between the parent drug and metabolites. With the mass defect window set at about ± 50 mDa from that of the parent drug, a significant number of background interference ions can be removed and the metabolite profile of biological sample can be obtained. In practice, Bateman et al. applied MDF successfully to detect and identify several new metabolites of indinavir [15]. Zhu et al. presented an improved MDF method employing both drug and core structure filter templates to detect the oxidative metabolites [16]. Zhang et al. presented an overview of various basic principles of MDF approach to detect drug metabolites [17]. In addition, application of MDF to detect herbal components was also reported by Yan et al.; however, it was limited in characterizing the mass defect profile by several standard compounds [8]. Theoretically, the compounds in TCM could be classified into several families and the components in the same family usually share the same carbon skeleton or substructures. Therefore, careful consideration of filter reference and corresponding substituents would be able to define a mass defect window for certain homologues components. Such a mass defect window can then be applied to exclude out the majority of non-related ions automatically and conveniently from the complex matrices. The resulting simplified data could facilitate the identification of structural analogues in TCMs. The present study thus used the powerful built-in MDF method to rapidly capture the characteristic structural analogues in complex herbal extract.

After screening the characteristic components in *Ophiopogon japonicus* extract based on LCMS-Q-TOF and the MDF technique, structural identification was further carried out to investigate the accuracy and efficiency of MDF. In this process, the hybrid ion trap and time-of-flight mass spectrometry (LCMS-IT-TOF) was applied to characterize both target and non-target components in *Ophiopogon japonicus* extract. LCMS-IT-TOF integrates the capabilities of IT and TOF along with LC for efficient separation in a single instrument, with the excellent MSⁿ function and sensitivity. Our previous research had systematically described its attractive merits in multi-components identification of TCM, including *Schisandra chinensis* extract [13], *Shengmai injection* [14], and *Mai-Luo-Ning injection* [18], as well as the metabolites identification of herbal medicines [19].

Herein, we described an efficient and generally applicable approach to identify compounds in *Ophiopogon japonicus* extract based on LCMS-Q-TOF and LCMS-IT-TOF. We highlighted the practical and reliable qualities of the MDF approach in the rapid analysis of ophiopogonins and ophiopogonones. Importantly, this methodology could be envisioned to exhibit a wide application for the identification of complicated components from various complex mixtures such as herbal preparations, biological, and environmental samples.

2. Experimental and methods

2.1. Reagents and chemicals

Authentic standard of ophiopogonin D (purity >99%) was purchased from Nanjing Zelan Corporation (Jiangsu China). HPLC-grade acetonitrile and methanol were purchased from Fisher Scientific (Fair Lawn, NJ, USA). All aqueous solutions were prepared with deionized water purified by a Milli-Q Ultrapure water system (Millipore, Bedford, USA). Solid phase extraction (SPE) cartridges (C₁₈, 500 mg/3 mL) were purchased from United Chemical Technologies Inc (Bristol, United States). Other chemicals and solvents were all of analytical grade. *Ophiopogon japonicus* tubers were purchased from the Xian Sheng Drug Store (Jiangsu, China) and the materials were cultivated in Sichuan province by authentication.

2.2. Plant material extraction and sample preparation

Ophiopogon japonicus tubers were authenticated according to morphological characteristics. The raw materials (1.0 g) were ultrasonicated twice for 120 min with 10 mL ethanol–water (v/v, 75:25). Then, the two extracts were combined, filtered and condensed under reduced pressure using a rotary evaporator. The residue was dissolved in 10 mL water.

Before analysis, the sample was pretreated by solid phase extraction (SPE) in order to remove the ophiopogon polysaccharide. Firstly, the SPE cartridges were activated with 2 mL of methanol, followed by 2 mL of water. Then, 200 μ L of extracts samples were applied to the cartridges manually and washed with 2 mL water. After drying, the cartridges were then eluted with 2 mL of methanol. The eluent was evaporated to dryness under nitrogen at 40 °C. The residue was reconstituted with 200 μ L of acetonitrile and then vortex mixed. A volume of 5 μ L aliquot was analyzed by LCMS-Q-TOF and LCMS-IT-TOF, respectively.

2.3. HPLC and MS conditions

HPLC: For analysis of the multi-components in *Ophiopogon japonicus*, the same type of Prominence HPLC system was coupled with hybrid quadrupole time-of-flight tandem mass spectrometry LCMS-Q-TOF (LCMS-Triple TOF 5600, AB SCIEX, Foster City, CA) and the ion trap time-of-flight mass spectrometry (LCMS-IT-TOF, Shimadzu Corporation, Kyoto, Japan), which equipped with an LC-20AB binary pump, an SIL-20AC autosampler, and a CTO-20AC column oven. Chromatographic separation was performed on C₁₈ reversed phase LC column (Phenomenex Luna, 5 μ m particles, 2.1 mm \times 150 mm). The mobile phase (delivered at 0.2 mL/min) consisted of solvent A, H₂O containing 0.02% acetic acid (v/v) and solvent B, acetonitrile containing 0.02% acetic acid (v/v). A binary gradient elution was employed for the separation, and the consecutive program was as follows: an isocratic elution of 25% solvent B for the initial 5 min, followed by a linear gradient elution of 25–75% solvent B from 5 to 55 min. After holding the composition of 75% solvent B for the next 3 min, the column was returned to its starting conditions until 65 min for column balance.

Q-TOF-MS: The samples were firstly analyzed in negative ionization mode by the LCMS-Q-TOF, a hybrid triple quadrupole time-of-flight mass spectrometer equipped with Turbo V sources and a Turbolonspray interface. The following MS conditions were used: ionspray voltage, 5.5 kV; declustering potential (DP), 70 V; the turbo spray temperature, 400 °C; nebulizer gas (Gas 1) of 50 psi; heater gas (Gas 2), 50 psi; curtain gas, 30 psi. Nitrogen was kept as nebulizer and auxiliary gas. The TOF MS scan was operated with the mass range of m/z 300–1500. Recalibration was carried by Easy-Mass Accuracy[®] device before analysis.

IT-TOF-MS: Fragmentation was carried out on the mass spectrometer of IT-TOF-MS equipped with an ESI source in negative ionization mode. The optimized analytical MS parameters were as follows: interface voltage -3.5 kV; nebulizing gas (N_2) flow, 1.5 L/min; drying gas pressure, 50 kPa; ion trap pressure, 1.7×10^{-2} Pa; ion accumulate time, 30 ms; the isolation width of precursor ions, 3.0 amu. Accurate mass determination was corrected by calibration using the sodium trifluoroacetate as reference. The analysis of ophiopogonins and ophiopogonones was achieved in two segmental experiments. For ophiopogonins analysis: scan ranges were set at m/z 500 – 1500 for MS^1 , 200 – 1300 for MS^2 ; 100 – 1000 for MS^3 ; ultra-high purity argon was used as the cooling gas and the collision gas for collision induced dissociation (CID), and the collision energy was set at 50% for MS^2 and 100% for MS^3 ; For ophiopogonones analysis: the spectra were recorded in the range of m/z 300 – 450 for MS^1 , m/z 50 – 400 for MS^2 , 50 – 300 for MS^3 ; and the collision energy was adjusted to 50% for MS^2 and 100% for MS^3 .

2.4. Mass defect filtering approach and formula prediction

MDF method was introduced to facilitate the detection of characteristic components which was dependent on a built-in setting by the Peak View SoftwareTM v. 1.1 (AB SCIEX, Foster City, CA). It was well-known that structural analogues in herbs usually shared with the similar core substructure, and characteristic compounds were generated via various chemical groups including hydroxyls, formyls, methoxys, methyls, glycosylations or combination of them. Each substituent possessed the relatively minor and defined changes in the mass defect of the core substructure. Therefore, the mass defect profile of the analogues usually changed within a limited range. Therefore, core substructure and different substituent combination were the two essential requirements to realize the MDF approach.

According to the theory above, the first step of the filter was to establish the filtering reference based on all the structures of the published components. The second step was to confirm the mass defect range according to the substitution of various constituents. Then, the filter chromatogram could be obtained according to the setting expressed as Central formula \pm mass defect tolerance. Central formula was equal to the average of maximum and minimum elements of ophiopogonins/ophiopogonones, and mass defect tolerance was equal to the half width of mass defects range. Once the filtering setting was applied to the chromatogram, the heterogeneous ions could be removed and characteristic ions remained visible.

The detected ions were then subjected to formula prediction. Parameters of the prediction of ophiopogonones were set as follows: the maximum tolerance of mass error was set at 5 ppm; H–C ratio was below 5 ; DBE (degree of unsaturation) was defined as 9 – 14 ; elemental composition ranged from 10 to 30 for carbon; from 10 to 30 for hydrogen; from 2 to 10 for oxygen. All the molecules were presumed to have no nitrogen. Parameters of the prediction of ophiopogonin: the maximum tolerance of mass error was set at 5 ppm; H–C ratio was below 5 ; DBE was defined between 7 and 15 ; elemental composition ranged from 20 to 65 for carbon; from 50 to 100 for hydrogen; from 0 to 30 for oxygen. All the molecules were presumed to have no nitrogen.

3. Results and discussion

3.1. Peaks detection for *Ophiopogon japonicus* extract by LCMS-Q-TOF

After the optimization of extraction procedure and sample preparation, a simple LCMS-Q-TOF method was developed to the

detect constituents in *Ophiopogon japonicus* extract. The total ion chromatogram (TIC) was shown in Fig. 1A, and most of the constituents were well separated under the gradient elution condition with high resolution and good sensitivity. However, matrices derived signals made finding characteristic compounds extremely challenging, and only few peaks could be distinguished from the background.

3.2. Establishment of MDF approach to detect the characteristic components

In the TIC of *Ophiopogon japonicus* extract, some components ions with low abundance were submerged in the background ions, leading to an easy miss of the compounds of interest during the manual inspection. In order to reduce the potential interferences of matrix ions and identify the characteristic compounds rapidly and globally, the MDF was applied to capture the characteristic peaks.

Ophiopogonone: Based on the concept of the MDF, the first step was the definition of the filter reference according to the core substructure. Ophiopogonones have the common skeleton of 3-benzyl chromone and it can be structurally classified into the homoisoflavanone and homoisoflavone by the degrees of unsaturation of C_2 and C_3 . Theoretically, the double bond in C_2 – C_3 sites made the mass defect of homoisoflavone smaller than that of corresponding homoisoflavanone. Consequently, the filter reference was determined as hydroxylated 3-benzyl chromone ($C_{16}H_{11}O_3$), as illustrated in Fig. 2A. The calculated mass defect was 0.0714 . The substituents of ophiopogonone were predominantly hydroxyls, formyls, methoxyls and methyls. It should be pointed out that methylenedioxy group corresponding to CO_2 attachment, usually linking to C_3' and C_4' , could be considered as two hydroxyl groups. According to the summary of the mass defects of the various substituents, both methyl groups and desaturation produced the maximum increase of mass defects; while only hydroxyl groups produced decrease. Therefore, the maximum number of four hydroxyl groups was assigned to obtain the minimum value of mass defect corresponding to $C_{16}H_{11}O_{27}$ and five methyl groups was assigned to obtain the maximum value corresponding to $C_{21}H_{23}O_4$. The calculated mass defect range was from 0.0510 to 0.1653 and the filter setting was determined as ($C_{18.5}H_{17}O_{5.5} \pm 55$ mDa) over the mass range of 300 – 400 Da. The generated chromatogram after filtration was displayed in Fig. 1B. Obviously, the noise level of the filtered chromatogram was about 0.5×10^4 counts per seconds (cps), and was much lower than that of the original chromatogram (1.0×10^6 cps, Fig. 1A). More importantly, 34 compounds were distinguished (see Table 1).

Ophiopogonin: The analysis of the ophiopogonin was more complex since the substitutions were much more complicated. Fig. 2B listed the main steroidal saponins in *Ophiopogon japonicus*, which mainly included spirostanol and furostanol glycosides. Overall, there were six types on the basis of the structures of different aglycones: diosgenin (spirostane + OH); rusco-genin (spirostane + 2OH); pennogenin (spirostane + 2OH); ophiopogonin (spirostane + 3OH); furostan [(spirostane + OH + $C_6H_{12}O_6$) or (spirostane + 2OH + $C_6H_{12}O_6$)]. Structurally, these glycosides had spirostane or its derivatives as their common skeleton, while the sugar moieties were oligosaccharides containing 1 – 4 types of sugar. Therefore, spirostane corresponding to $C_{27}H_{41}O_2$ was defined as the filter reference. The calculated mass defect was 0.3112 .

The second critical step was to determine the mass defect range based on the filter reference and different substituent combination. All kinds of ophiopogonins were generated via different hydroxyls and glycosyls. As shown in Fig. 2C, only hydroxyl groups made negative contribution to the mass defect. Besides, among the conjugated sugars, the substitution of deoxyheose produced the maximum increase of the mass defect, and the substitution of

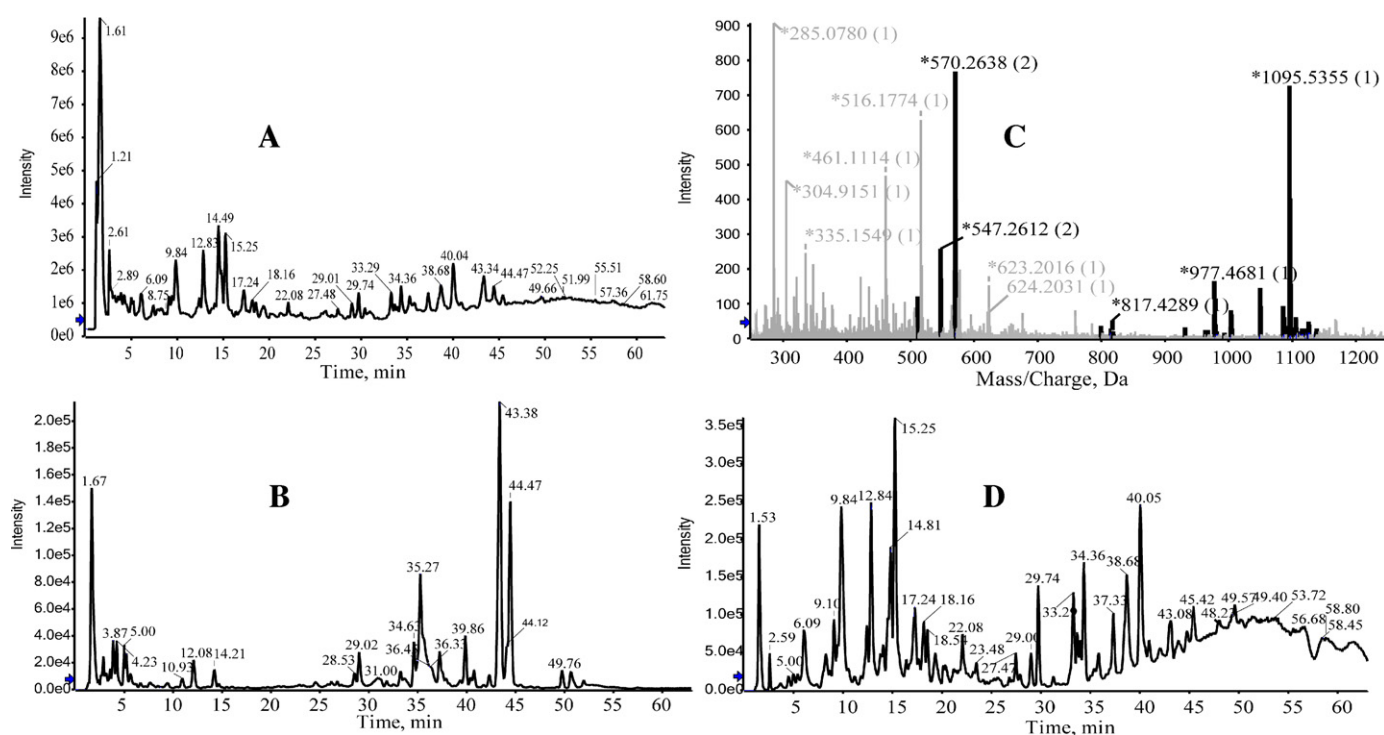


Fig. 1. The unfiltered TIC obtained by LCMS-Q-TOF (A) and the corresponding filtered chromatogram of ophiopogonones (B) and ophiopogonins (D) obtained by MDF filtration. (C) The representative mass spectrum (retention time: 9.034 min). After the processing by MDF, the majority of ions (gray) in background were filtered out, and the characteristic ions of ophiopogonins (black) appeared.

pentose produced the minimum increase. Therefore, the mass defect of ophiopogonin (spirostane + 3OH) was minimal among the six types. Assignment of three hydroxyl groups and a pentose group was to produce the minimum mass defect corresponding to the formula of $C_{32}H_{49}O_9$ which was 0.3379 of mass defect by calculation. Furostan (spirostane + OH + $C_6H_{12}O_6$) had the maximum mass defect since an extra glucose unit ($C_6H_{12}O_6$) was attached on C_{26} position. So, one hydroxyl group, one pentose and four deoxyheoses were assigned on the filter reference to obtain the maximum mass defect with the formula of $C_{61}H_{95}O_{26}$. The calculated mass defect value was 0.6024. Then, the produced mass defect ranges, converting into the setting of $(C_{46.5}H_{72}O_{17.5} \pm 136 \text{ mDa})$ over the mass range of 600–1500 Da, was applied to detect the ophiopogonins.

As shown in the unfiltered chromatogram, the noise level was at about $1 \times 1.0e^6$ cps, which presented a great challenge to find

the low constituents. After filtration by the MDF technique, all irrelevant ions in mass spectrum, of which the mass defects were not within the filter windows, were excluded firmly (see Fig. 1C). Consequently, the de-protonated molecules of the interest became predominant ions in the TIC (see Fig. 1D). It was anticipated that a total of 62 peaks attributed to ophiopogonins were detected in a 65 min chromatographic run (see Table 2).

3.3. Accuracy evaluation of MDF approach by structural inference using LCMS-IT-TOF

The effectiveness of the MDF approach using core substructure as filter reference was well demonstrated both for ophiopogonins and ophiopogonones in *Ophiopogon japonicus* extract. Next, we investigated the accuracy of the MDF approach from the MSⁿ

Table 1
Detection of ophiopogonones by the MDF approach.

No.	Rt (min)	Measurement (ppm)	Predicted formula	No.	Rt (min)	Measurement (ppm)	Predicted formula
1 ^a	3.9	337.0929 (0.0)	$C_{16}H_{17}O_8$	18	35.3	359.1139 (0.8)	$C_{19}H_{19}O_7$
2 ^a	5.1	337.0931 (0.6)	$C_{16}H_{17}O_8$	19	35.6	357.0975 (−1.3)	$C_{19}H_{17}O_7$
3 ^a	11.0	345.0975 (−1.4)	$C_{18}H_{17}O_7$	20	36.4	343.1180 (−2.1)	$C_{19}H_{19}O_6$
4 ^a	12.1	312.1245 (1.2)	$C_{18}H_{18}NO_4$	21	37.2	343.1190 (0.8)	$C_{19}H_{19}O_6$
5 ^a	14.2	312.1245 (1.2)	$C_{18}H_{18}NO_4$	22	37.6	355.0827 (1.1)	$C_{19}H_{15}O_7$
6	26.8	345.0984 (1.2)	$C_{18}H_{17}O_7$	23	37.9	341.1036 (1.6)	$C_{19}H_{17}O_6$
7	28.5	327.0880 (2.1)	$C_{18}H_{15}O_6$	24	39.7	357.1343 (−0.2)	$C_{20}H_{21}O_6$
8	29.0	373.1294 (0.3)	$C_{20}H_{21}O_7$	25	39.8	325.0719 (0.4)	$C_{18}H_{13}O_6$
9	29.2	359.1137 (0.2)	$C_{19}H_{19}O_7$	26	39.9	327.0880 (1.8)	$C_{18}H_{15}O_6$
10	31.2	339.0875 (0.3)	$C_{19}H_{15}O_6$	27	40.8	313.1091 (3.0)	$C_{18}H_{17}O_5$
11	31.9	325.1076 (−1.7)	$C_{19}H_{17}O_5$	28	42.3	339.0877 (0.8)	$C_{19}H_{15}O_6$
12	28.5	329.1033 (0.7)	$C_{18}H_{17}O_6$	29	43.3	325.1081 (−0.1)	$C_{19}H_{17}O_5$
13	33.3	373.1294 (0.3)	$C_{20}H_{21}O_7$	30	43.4	341.1037 (1.9)	$C_{19}H_{17}O_6$
14	33.6	313.1084 (0.8)	$C_{18}H_{17}O_5$	31	44.5	327.1241 (0.9)	$C_{19}H_{19}O_5$
15	34.0	341.0665 (−0.5)	$C_{18}H_{13}O_7$	32	49.8	353.0669 (0.6)	$C_{19}H_{13}O_7$
16	34.6	343.1190 (0.8)	$C_{19}H_{19}O_6$	33	50.7	355.0824 (0.2)	$C_{19}H_{15}O_7$
17	34.7	341.0664 (−0.8)	$C_{18}H_{13}O_7$	34	50.9	339.0876 (−0.6)	$C_{19}H_{15}O_6$

^a Heterogeneous peaks because of their distinctive eluted time.

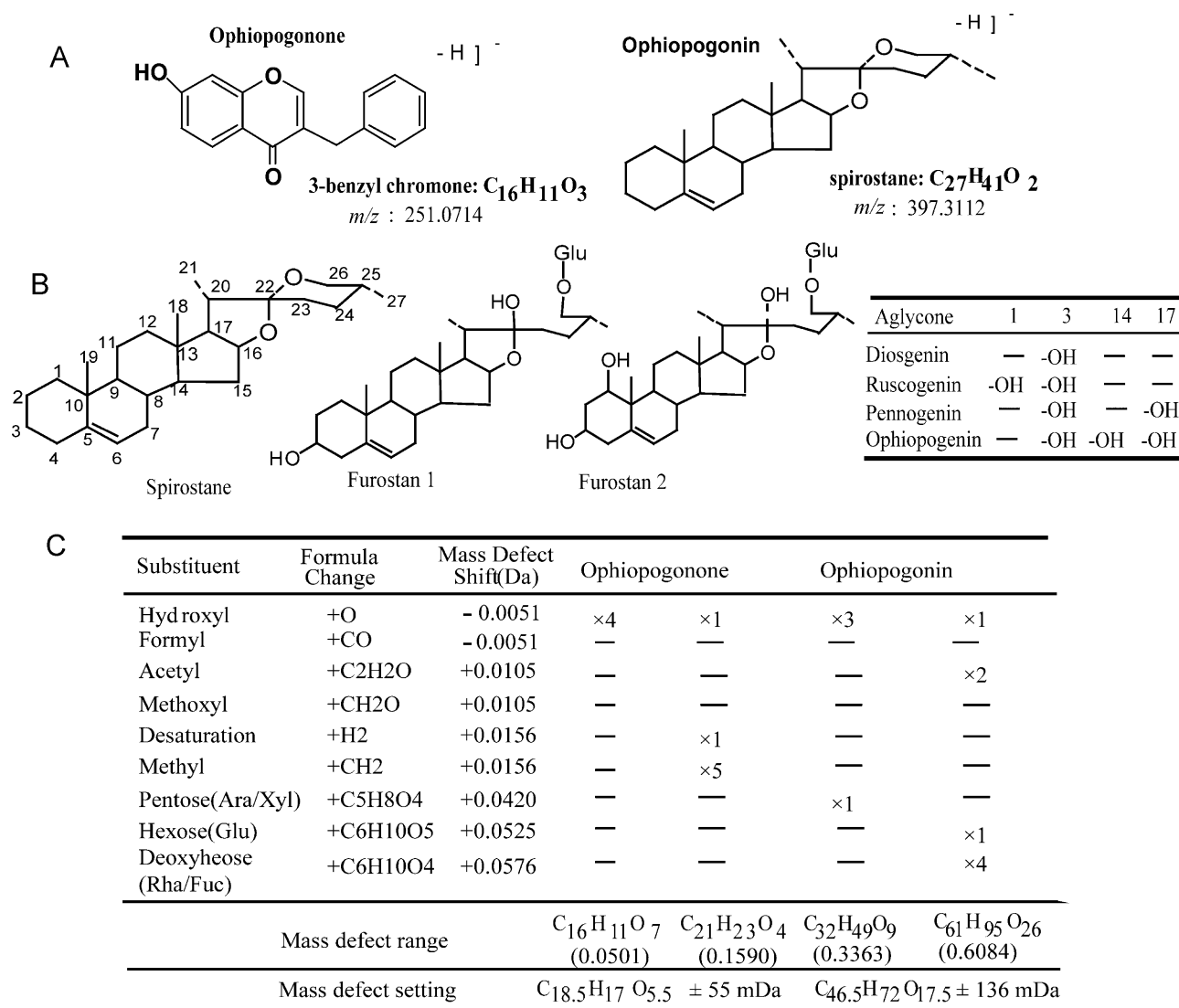


Fig. 2. The proposed MDF approach with predefined filter reference (A) and substituents (C). The main substructures of ophiopogonins (B).

fragmentation of view using LCMS-IT-TOF platform. The capability of MSⁿ fragmentation and mass accuracy of each MSⁿ stage made LCMS-IT-TOF an attractive tool for structural inference. Therefore, the accuracy of screening results based on MDF approach was investigated by the MSⁿ fragmentation analysis provided by LCMS-IT-TOF. It should be noted that, to ensure the unbiased analysis in two mass spectrometer systems, the same HPLC conditions were used. Except for the retention time and the peak shape, accurate mass was a third important parameter to identify the compounds detected by the two platforms (ppm < 5).

3.3.1. Structural identification of ophiopogonones

Target analysis with predefined fragmentation: On the basis of the previous researches [20,21], ophiopogonones could be structurally divided into four classes as demonstrated in Fig. 3. For type i homoisoflavone, where the C₂–C₃ was connected by a double bond, the [M–H][–] ions appeared to be stable. They could lose B-ring according to the cleavage of C₉–C₁ and C₉–C₃, yielding two product ions which typically differed 13 Da. This characteristic mass difference could be used as indication of type i. Homoisoflavonones of type ii and iii, containing saturated C₂–C₃ bonds, usually undertook successive loss of B-ring from the fission of C₃–C₉ and then a molecule CO at the C₄ position. The characteristic mass difference of

the two product ions was 28 Da, which could be used to discern the types of homoisoflavonones; for type iv ophiopogonone which carried a formyl group in A-ring, fragmentation was always triggered by the loss of CO molecule to form the product ion [M+H–CO][–] irrespective whether the C₂–C₃ bond was saturated or not. In addition, methoxylated homoisoflavonoid could lead to the loss of 15 mass units. Based on the above MS fragmentation rules, a total of 20 target ophiopogonones was identified successfully. All structures were summarized in Fig. 4 and MSⁿ information was illustrated in Supplementary Information.

Non-target analysis: Among the 14 unknown peaks of ophiopogonones, the first eluted five peaks were considered as heterogeneous compounds by the consideration of their distinctive chromatographic behaviors. These heterogeneous peaks had high polarity which eluted at 3–14 min, being different from others which eluted at 26–50 min. This was also consistent with the previous research reported by Lin et al. [21]. Except for these five peaks, the others were all considered as the potential ophiopogonones. These non-targets could not be detected by the conventional screen which was highly dependent on the predefined fragments or neutral loss information. For the remaining 9 non-targets, two were failed to identify since its low intensity and insufficient MSⁿ information.

Table 2
Detection of ophiopogonins by the MDF approach.

No.	Rt (min)	Measurement ^b (ppm)	Predicted formula	No.	Rt (min)	Measurement (ppm)	Predicted formula
35	6.1	1095.5190 (−0.9) 1141.5222 (−0.5)	C ₅₁ H ₈₃ O ₂₅ C ₅₂ H ₈₅ O ₂₇	51	17.4	959.4863 (0.6) 1005.4913 (0.1)	C ₄₇ H ₇₅ O ₂₀ C ₄₈ H ₇₇ O ₂₂
36	8.7	1211.5650 (−0.4) 1257.5680 (−0.3)	C ₅₆ H ₉₁ O ₂₈ C ₅₇ H ₉₃ O ₃₀	52	17.7	1033.5226 (0.1) 1079.5286 (0.6)	C ₅₀ H ₈₁ O ₂₂ C ₅₁ H ₈₃ O ₂₄
37	9.0	1211.5650 (−0.1) 1257.5680 (−0.3)	C ₅₆ H ₉₁ O ₂₈ C ₅₇ H ₉₃ O ₃₀	53	18.5	901.4804 (0.2) 947.4860 (0.3)	C ₄₅ H ₇₃ O ₁₈ C ₄₆ H ₇₅ O ₂₀
38	9.8	1079.5287 (0.7) 1125.5341 (0.6)	C ₅₁ H ₈₃ O ₂₄ C ₅₂ H ₈₅ O ₂₆	54	19.2	923.4646 (−1.6) 969.4691 (−1.0)	C ₄₇ H ₇₁ O ₁₈ C ₄₈ H ₇₃ O ₂₀
39	10.0	933.4697 (−0.4) 979.4760 (0.5)	C ₄₅ H ₇₃ O ₂₀ C ₄₆ H ₇₅ O ₂₂	55	19.6	1031.5063 (−0.5) 1077.5116 (−0.7)	C ₅₀ H ₇₉ O ₂₂ C ₅₁ H ₈₁ O ₂₄
40	11.8	1049.5168 (−0.6) 1095.5223 (−0.5)	C ₅₀ H ₈₁ O ₂₃ C ₅₁ H ₈₃ O ₂₅	56	20.0	899.4638 (−0.9) 945.4697 (−0.4)	C ₄₅ H ₇₁ O ₁₈ C ₄₆ H ₇₃ O ₂₀
41	12.4	1049.5176 (0.2) 1095.5235 (0.6)	C ₅₀ H ₈₁ O ₂₃ C ₅₁ H ₈₃ O ₂₅	57	20.4	1075.5320 (−1.0) 1121.538 (−0.5)	C ₅₂ H ₈₃ O ₂₃ C ₅₃ H ₈₅ O ₂₅
42	12.8	917.4753 (0.2) 963.4814 (0.8)	C ₄₅ H ₇₃ O ₁₉ C ₄₆ H ₇₅ O ₂₁	58	21.2	1177.5638 (−0.8) 1223.5696 (−0.5)	C ₅₆ H ₈₉ O ₂₆ C ₅₇ H ₉₁ O ₂₈
43	12.2	917.4746 (−0.6) 963.4809 (0.3)	C ₄₅ H ₇₃ O ₁₉ C ₄₆ H ₇₅ O ₂₁	59	22.1	1045.5225 (0.6) 1091.5282 (0.2)	C ₅₁ H ₈₁ O ₂₂ C ₅₂ H ₈₃ O ₂₄
44	14.1	1195.5741 (−1.0) 1241.5798 (−0.8)	C ₅₆ H ₉₁ O ₂₇ C ₅₇ H ₉₃ O ₂₉	60	22.7	1117.5416 (−1.8) 1163.5487 (−0.4)	C ₅₄ H ₈₅ O ₂₄ C ₅₅ H ₈₇ O ₂₆
45	14.5	1195.5754 (0.1) 1241.5774 (−0.2)	C ₅₆ H ₉₁ O ₂₇ C ₅₇ H ₉₃ O ₂₉	61	23.5	1117.5428 (−0.7) 1163.5488 (−0.3)	C ₅₄ H ₈₅ O ₂₄ C ₅₅ H ₈₇ O ₂₆
46	14.8	1063.5321 (−0.9) 1109.5385 (0.0)	C ₅₁ H ₈₃ O ₂₃ C ₅₂ H ₈₅ O ₂₅	62	26.8	901.4430 (−0.9) 947.4492 (−0.1)	C ₄₄ H ₆₉ O ₁₉ C ₄₅ H ₇₁ O ₂₁
47	15.3	1063.5328 (−0.2) 1109.5386 (0.1)	C ₅₁ H ₈₃ O ₂₃ C ₅₂ H ₈₅ O ₂₅	63 ^a	22.3	967.4158 (3.9)	C ₄₇ H ₆₇ O ₂₁
48	15.7	959.4827 (−0.9) 1005.4909 (−0.3)	C ₄₇ H ₇₅ O ₂₀ C ₄₈ H ₇₇ O ₂₂	64	27.5	769.4016 (−1.2) 815.4069 (−0.2)	C ₃₉ H ₆₁ O ₁₅ C ₄₀ H ₆₃ O ₁₇
49	16.4	1061.5184 (0.9) 1107.5236 (0.6)	C ₅₁ H ₈₁ O ₂₃ C ₅₂ H ₈₃ O ₂₅	65	27.9	753.4057 (−1.3) 799.4116 (−0.7)	C ₃₉ H ₆₁ O ₁₄ C ₄₀ H ₆₃ O ₁₆
50	17.3	1237.5867 (0.7) 1283.5922 (0.6)	C ₅₈ H ₉₃ O ₂₈ C ₅₉ H ₉₅ O ₃₀	66	29.0	885.4480 (−1.1) 931.4538 (−0.7)	C ₄₄ H ₆₉ O ₁₈ C ₄₅ H ₇₁ O ₂₀
67	29.7	753.4064 (−0.4) 799.4125 (−0.4)	C ₃₉ H ₆₁ O ₁₄ C ₄₀ H ₆₃ O ₁₆	82	39.0	911.4643 (−0.3) 957.4691 (−1.0)	C ₄₆ H ₇₁ O ₁₈ C ₄₇ H ₇₃ O ₂₀
68 ^a	25.8	981.4359 (2.31)	C ₄₄ H ₇₀ O ₂₄	83	40.0	853.4577 (−1.7) 899.4642 (−0.4)	C ₄₄ H ₆₉ O ₁₆ C ₄₅ H ₇₁ O ₁₈
69	31.3	927.4578 (−1.8) 973.4645 (−0.5)	C ₄₆ H ₇₁ O ₁₉ C ₄₇ H ₇₃ O ₂₁	84	40.2	779.4210 (−1.7) 825.4268 (−1.2)	C ₄₁ H ₆₃ O ₁₄ C ₄₂ H ₆₅ O ₁₆
70	33.0	927.4580 (−1.6) 973.4644 (−0.6)	C ₄₆ H ₇₁ O ₁₉ C ₄₇ H ₇₃ O ₂₁	85	40.2	953.4734 (−1.8) 999.4798 (−0.8)	C ₄₈ H ₇₃ O ₁₉ C ₄₉ H ₇₅ O ₂₁
71	33.3	869.4531 (−1.1) 915.4594 (−0.1)	C ₄₄ H ₆₉ O ₁₇ C ₄₅ H ₇₁ O ₁₉	86	40.9	853.4585 (−0.7) 899.4643 (−0.3)	C ₄₄ H ₆₉ O ₁₆ C ₄₅ H ₇₁ O ₁₈
72	33.7	795.4168 (−0.6) 841.4230 (0.3)	C ₄₁ H ₆₃ O ₁₅ C ₄₂ H ₆₅ O ₁₇	87	42.0	721.4153 (−2.2) 767.4223 (−1.2)	C ₃₉ H ₆₁ O ₁₂ C ₄₀ H ₆₃ O ₁₄
73	34.4	737.4106 (−1.6) 783.4169 (−0.4)	C ₃₉ H ₆₁ O ₁₃ C ₄₀ H ₆₃ O ₁₅	88	43.1	721.4163 (−0.8) 767.4208 (−2.0)	C ₃₉ H ₆₁ O ₁₂ C ₄₀ H ₆₃ O ₁₄
74	35.0	737.4109 (−1.2) 783.4172 (−1.1)	C ₃₉ H ₆₁ O ₁₃ C ₄₀ H ₆₃ O ₁₅	89	43.1	895.4696 (−0.1) 941.4747 (−0.5)	C ₄₆ H ₇₁ O ₁₇ C ₄₇ H ₇₃ O ₁₉
75	35.2	795.4160 (−1.6) 841.4224 (−0.4)	C ₄₁ H ₆₃ O ₁₅ C ₄₂ H ₆₅ O ₁₇	90	44.5	953.4739 (−1.3) 999.4802 (−0.4)	C ₄₈ H ₇₃ O ₁₉ C ₄₉ H ₇₅ O ₂₁
76	35.5	969.4683 (−1.8) 1015.4747 (−0.8)	C ₄₈ H ₇₃ O ₂₀ C ₄₉ H ₇₅ O ₂₂	91	44.8	895.469 (−0.8) 941.475 (−0.2)	C ₄₆ H ₇₁ O ₁₇ C ₄₇ H ₇₃ O ₁₉
77	35.8	911.4633 (−1.4) 957.4688 (−1.3)	C ₄₆ H ₇₁ O ₁₈ C ₄₇ H ₇₃ O ₂₀	92	45.4	895.4688 (−1.0) 941.4744 (−0.8)	C ₄₆ H ₇₁ O ₁₇ C ₄₇ H ₇₃ O ₁₉
78	37.0	839.4427 (−0.9) 885.4483 (−0.7)	C ₄₃ H ₆₇ O ₁₆ C ₄₄ H ₆₉ O ₁₈	93	47.3	937.4812 (1.0) 983.4851 (−0.6)	C ₄₈ H ₇₃ O ₁₈ C ₄₉ H ₇₅ O ₂₀
79	37.3	911.4631 (−1.6) 957.4694 (−0.7)	C ₄₆ H ₇₁ O ₁₈ C ₄₇ H ₇₃ O ₂₀	94	48.1	763.4261 (−1.7) 809.4326 (−0.4)	C ₄₁ H ₆₃ O ₁₃ C ₄₂ H ₆₅ O ₁₅
80	38.7	779.4207 (−2.1) 825.4276 (−0.3)	C ₄₁ H ₆₃ O ₁₄ C ₄₂ H ₆₅ O ₁₆	95	49.6	937.4797 (−0.6) 983.4854 (−0.3)	C ₄₈ H ₇₃ O ₁₈ C ₄₉ H ₇₅ O ₂₀
81	39.0	851.4421 (−1.6) 897.4481 (−0.9)	C ₄₄ H ₆₇ O ₁₆ C ₄₅ H ₆₉ O ₁₈	96	49.7	937.4785 (−1.9) 983.4850 (−0.7)	C ₄₈ H ₇₃ O ₁₈ C ₄₉ H ₇₅ O ₂₀

^a Heterogeneous peaks because of their different ionization behavior.^b ophiopogonins can be detected as [M−H][−] and [M+HCOOH][−] in negative ionized mode.

For peak 6, deprotonated molecular ion [M−H][−] at *m/z* 345.0957 produced the predominant fragment ion at *m/z* 223.0606 ([M−H−C₇H₆O₂][−]) and *m/z* 169.0467 ([M−H−C₃H₃O₂−C₇H₆O₂][−]) which attributed to the loss of B-ring and C-ring, respectively. Extra loss of two atoms of oxygen suggested that two hydroxyl groups were substituted in B-ring. An abundant demethylated product at *m/z* 208.0306 was also observed (15 Da less than the ion at *m/z* 223.0598). It suggested that a methoxyl

group was presented in A-ring. Thus, peak 6 was identified as 5,7,2',4'-tetrahydroxy-8-methoxy-6-methyl homoisoflavanone. For peak 9, the major product ions at *m/z* 169.0519, 208.0373, 222.0619 and 344.0889 were the same with that of peak 6. Therefore, peak 9 might be characterized as 5,7,2'-trihydroxy-8,4'-dimethoxy-6-methyl homoisoflavanone.

Peak 8 gave the [M−H][−] ion at *m/z* 373.1294 in MS¹ spectrum. The MS² spectrum yielded prominent ions at *m/z* 183.0669 and

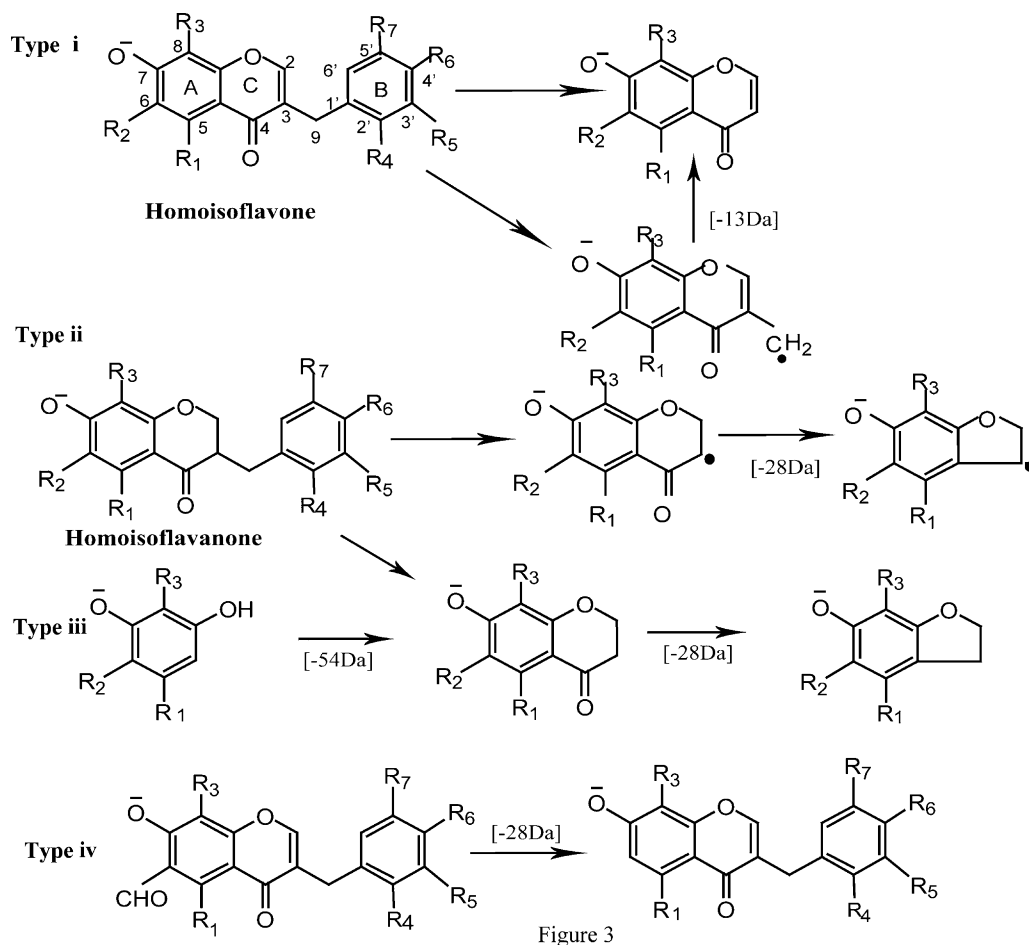


Fig. 3. The main fragmentation pathway for structural identification of ophiopogonones.

222.0531 corresponding to $[\text{C}_9\text{H}_{11}\text{O}_4]^-$ and $[\text{C}_{11}\text{H}_{10}\text{O}_5]^-$, which were mainly derived from the successive loss of B-ring and C-ring. By the analysis of the fragmental pathway, we could conclude peak 8 as the compound of 7,2'-dihydroxy-5,8,4'-trimethoxy-6-methyl homoisoflavanone.

Peak 29 gave the $[\text{M}-\text{H}]^-$ ion at m/z 325.1081. A high intensity ion at m/z 310.0845 could be attributed to the loss of a methyl radical. The minor response at m/z 281.0766 indicated the loss of methoxy group and methyl radical. According to the database search, peak 29 might be concluded as methyllophiopogonone B.

The deprotonated molecular ion of peak 18, eluting at 35.3 min, was at m/z 359.1112, and was as same as peak 9 ($t_R = 29.2$ min). The predominated fragment ion of peak 18 was at m/z 237.0764 obtaining by the loss of B-ring in MS^2 spectra which could also found from peak 9. The produced ions at m/z 326.0775 and m/z 344.0828, differing 18 Da, derived from the successive loss of CH_3 and H_2O , which strongly suggested an extra hydroxyl group in C₂. This peak was tentatively identified as 2,5,7,3'-tetrahydroxy-4'-methoxy-6,8-dimethyl homoisoflavanone, which was the first report in this study. Additionally, peak 11 and 12 could yield the product ion at m/z 295.0648, indicating the same or similar substructure was presented. These two peaks were initially concluded as 5-hydroxy-3', 4'-methylenedioxy-7-methoxy-8-methyl homoisoflavone and 5-hydroxy-7,4'-dimethoxy-8-methyl homoisoflavone.

3.3.2. Structural identification of ophiopogonins

Target analysis with predefined diagnostic fragment ions: To speed up our analysis of ophiopogonins, components were grouped and

identified according to diagnostic ions techniques referred to our previous publication. In our laboratory, Zheng et al. proposed a "diagnostic fragment ion based extension strategy (DFIBES)" for rapid screening and identification of structural analogues in *Shen-mai injection* [14]. DFIBES was originally proposed from the fact that the components contained in TCMS could usually be structurally classified into several subfamilies and components of the same family usually contained the same carbon skeleton or substructures, from which the same fragment ions could be defined as diagnostic fragment ions (DFIs). And then these well defined DFIs were used to screen and identify the analogues. Herein we applied such a strategy to classify and identify the potential ophiopogonins.

Generally, the fragmentation patterns of steroid saponin were mainly derived from the fission of glucosidic bonds. The obtained neutral loss could be used for elucidation of sugar moiety. For spirostanol glycosides, the aglycone moiety was difficult to fragment in collision-induced dissociation (CID). The elimination of sugar could be considered as the only useful information for ophiopogonins identification, and $[\text{M}-\text{H}+\text{monosaccharide}]^-$ could be used as DFIs. By the investigation of the different structures, spirostanol glycosides were roughly classified into three subgroups based on the different DFIs (see Fig. 5). For type I, the DFIs were determined as m/z 591.3535 ($\text{C}_{33}\text{H}_{51}\text{O}_9$) corresponding to $[\text{ruscogenin}-\text{H}+\text{C}_6\text{H}_{10}\text{O}_5]^-$ or $[\text{pennogenin}-\text{H}+\text{C}_6\text{H}_{10}\text{O}_5]^-$ and m/z 737.4115 ($\text{C}_{39}\text{H}_{61}\text{O}_{13}$) corresponding to $[\text{ruscogenin}-\text{H}+\text{C}_6\text{H}_{10}\text{O}_5+\text{C}_6\text{H}_{10}\text{O}_4]^-$ or $[\text{pennogenin}-\text{H}+\text{C}_6\text{H}_{10}\text{O}_5+\text{C}_6\text{H}_{10}\text{O}_4]^-$. Similarly, for type II, the DFIs were determined as m/z 575.3586 ($\text{C}_{33}\text{H}_{51}\text{O}_8$) corresponding to $[\text{diosgenin}-\text{H}+\text{C}_6\text{H}_{10}\text{O}_5]^-$ or

NO	Types	R1	R2	R3	R4	R5	R6	R7	R8
Targets									
15	A	-OH	-CH3	-OH	-H	-OH	-O-CH2-O-		-H
17	A	-OH	-H	-OH	-CH3	-OH	-O-CH2-O-		-H
22	A	-OH	-CH3	-OH	-CH3	-OH	-O-CH2-O-		-H
23	A	-OH	-CH3	-OCH3	-H	-H	-OH	-OCH3	-H
25	A	-OH	-H	-OH	-CH3	-H	-O-CH2-O-		-H
28	A	-OH	-CH3	-OH	-CH3	-H	-O-CH2-O-		-H
24	B	-OH	-CH3	-OH	-CH3	-OCH3	-H	-OCH3	-H
26	B	-OH	-H	-OH	-CH3	-H	-O-CH2-O-		-H
27	B	-OH	-CH3	-OH	-H	-H	-H	-OCH3	-H
30	B	-OH	-CH3	-OH	-CH3	-H	-O-CH2-O-		-H
31	B	-OH	-CH3	-OH	-CH3	-H	-H	-OCH3	-H
13	B	-OH	-CH3	-OH	-CH3	-H	-OCH3	-OH	-OCH3
14	B	-OH	-CH3	-OH	-H	-H	-H	-OCH3	-H
16	B	-OH	-CH3	-OCH3	-H	-OCH3	-H	-OH	-H
19	C	-OH	-CH3	-OH	-CH3	-H	-O-CH2-O-		-H
20	B	-OH	-CH3	-OH	-CH3	-H	-H	-OH	-OCH3
21	B	-OH	-H	-OCH3	-CH3	-H	-H	-OH	-OCH3
32	A	-OH	-CHO	-OH	-CH3	-H	-O-CH2-O-		-H
33	B	-OH	-CHO	-OH	-CH3	-H	-O-CH2-O-		-H
34	A	-OH	-CHO	-OH	-CH3	-H	-H	-OCH3	-H
Non-targets									
6	B	-OH	-CH3	-OH	-OCH3	-OH	-H	-OH	-H
8	B	-OCH3	-CH3	-OH	-OCH3	-OH	-H	-OCH3	-H
9	B	-OH	-CH3	-OH	-OCH3	-OH	-H	-OCH3	-H
10	A	-OH	-H	-OCH3	-CH3	-H	-O-CH2-O-		-H
11	A	-OH	-H	-OCH3	-CH3	-H	-OCH3	-H	-H
18	C	-OH	-CH3	-OH	-CH3	-H	-OH	-OCH3	-H
29	A	-OH	-CH3	-OH	-CH3	-H	-H	-OCH3	-H

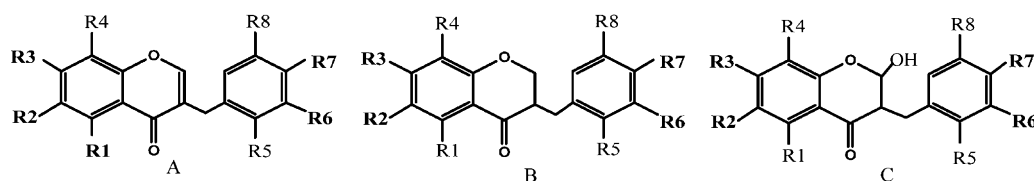


Fig. 4. The identification of ophiopogonones based on the predefined fragmentation.

[ruscogenin-H+C₆H₁₀O₄]⁻ and m/z 721.4166 (C₃₉H₆₁O₁₂) corresponding to [diosgenin-H+C₆H₁₀O₅+C₆H₁₀O₄]⁻ or [ruscogenin-H+2C₆H₁₀O₄]⁻. For type III, the DFIs were determined as m/z 445.2956 (C₂₇H₄₁O₅) corresponding to [ophiopogonin-H]⁻, m/z 607.3484 (C₃₃H₅₁O₁₀) corresponding to [ophiopogonin-H+C₆H₁₀O₅]⁻ and/or m/z 753.4064 (C₃₉H₆₁O₁₄) corresponding to [ophiopogonin-H+C₆H₁₀O₅+C₆H₁₀O₄]⁻. Differently, type IV and type V, which belonged to furostanol glycosides, both contained a glucose unit attached on the C₂₆ hydroxyl of the aglycone [22,23]. This glucose unit could be lost in CID and converted into their corresponding spirostanol glycosides by loss of a neutral molecule of C₆H₁₂O₆ (180 Da). Therefore, for type IV, the DFIs were determined as m/z 429.3007 (C₂₇H₄₁O₄) corresponding to [ruscogenin-H]⁻, m/z 591.3535 (C₃₃H₅₁O₉) corresponding to [ruscogenin-H+C₆H₁₀O₅]⁻ and m/z 771.4169 (C₃₉H₆₃O₁₅) corresponding to [furostan-H+C₆H₁₀O₅]⁻; for type V, the DFIs were determined as m/z 413.3058 (C₂₇H₄₁O₃) corresponding to [diosgenin-H]⁻, m/z 575.3586 (C₃₃H₅₁O₈) corresponding to [diosgenin-H+C₆H₁₀O₅]⁻ and m/z 755.4220 (C₃₉H₆₃O₁₄) corresponding to [furostan-H+C₆H₁₀O₅]⁻. With these DFIs, the aglycone could be easily identified. Then the saccharine moiety could be inferred from the mass difference between fragment ions. For example, the mass difference of 162 Da indicated the loss of glucosyl, and the mass difference of 146 Da indicated the

elimination of rhamnosyl or fucosyl. As a result, a total of 46 compounds were structural characterized (see Fig. 6).

Non-target analysis: After structural identification of target ophiopogonins according to their DFIs, there were still 16 ophiopogonins that could not produce DFIs. Except for peak 63 and 68, others gave both deprotonated ion [M-H]⁻ and adduct ion [M+HCOOH-H]⁻. It was an important indicator to potential steroid saponin. Although without predefined fragments, attempts were still made to structural characterization of these non-target compounds.

For peak 81, adduct ion [M+HCOOH-H]⁻ at m/z 897.4440 and low abundant deprotonated molecular ion [M-H]⁻ at m/z 851.4413 were observed simultaneously. In the MS² spectrum, the fragment ions [M-H-C₅H₈O₄]⁻ at m/z 719.3956 and [M-H-C₅H₈O₄-C₆H₁₀O₄]⁻ at m/z 573.3458 could be attributed to the successive loss of pentose and deoxyheose. It suggested that peak 81 belonged to neoruscogenin glycoside which had the same substructure with ruscogenin glycoside, except for the double bond in C₂₅-C₂₇. The final identification was (1 β ,3 β)-3-hydroxyspirosta-5,25(27)-dien-1-yl O-6-deoxy- α -L-mannopyranosyl-(1 \rightarrow 2)-O-[β -D-xylopyranosyl-(1 \rightarrow 4)]- β -D-glucopyranoside. Similarly, the [M-H]⁻ ion at m/z 899.4580 of peak 56 gave the product ions at m/z 753.4012 and 573.3340, corresponding to [M-H-C₆H₁₀O₄]⁻ and

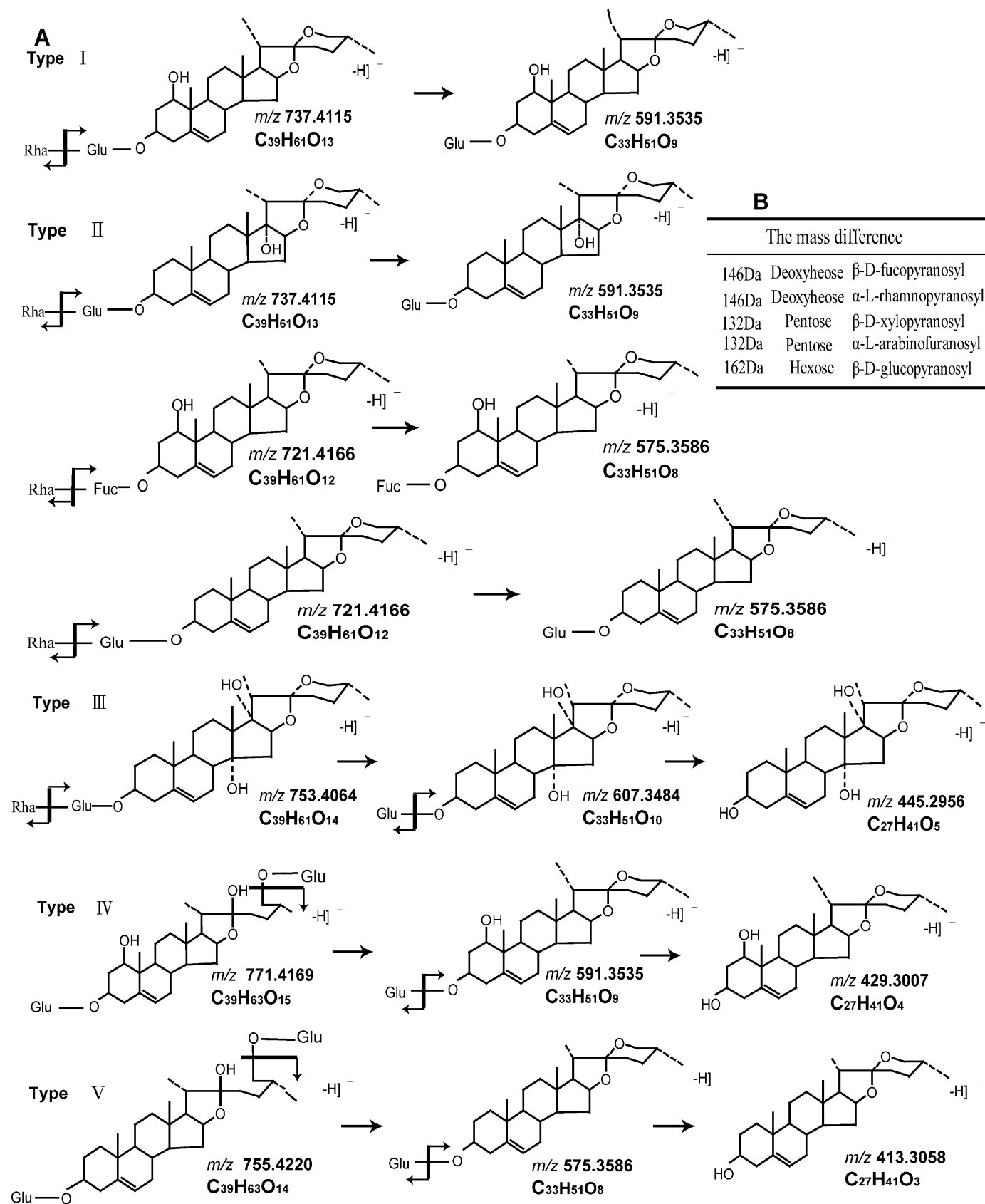
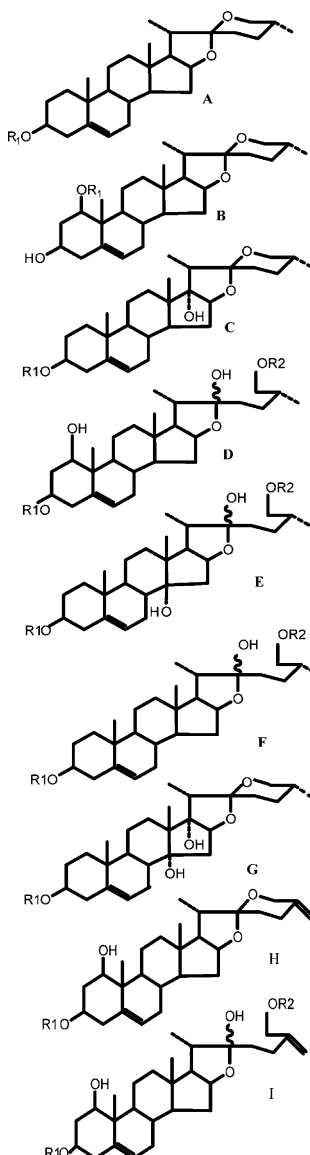


Fig. 5. The main fragmentation pathway for structural identification of ophiopogonins (A); the indicating mass difference between the product ions for sugar moiety (B).



No	Type	R1	R2
DFI: <i>m/z</i> 737.41; 591.35			
71	B	Rha—Glc— Xyl	
73	B	Rha—Glc—	
74	C	Rha—Glc—	
77	B	Acetyl—Glc—Fuc— Xyl	
79	C	Acetyl—Rha—Glc— Xyl	
82	C	Acetyl—Rha—Glc— Xyl	
80	B	Acetyl—Glc—Fuc—	
84	C	Acetyl—Rha—Glc—	
85	B	2Acetyl—Glc—Fuc— Xyl	
90	C	2Acetyl—Rha—Glc— Xyl	
DFI: <i>m/z</i> 721.42; 575.36			
83*	B	Rha—Fuc— Xyl	
86	A	Rha—Glc— Xyl	
87	B	Rha—Fuc—	
88	A	Rha—Glc—	
89	B	Acetyl—Rha—Fuc— Xyl	
91	A	Acetyl—Rha—Glc— Xyl	
92	A	Acetyl—Rha—Glc— Xyl	
94	B	Acetyl—Rha—Fuc—	
93	B	2Acetyl—Rha—Fuc—	
95	A	2Acetyl—Rha—Fuc—	
96	A	2Acetyl—Rha—Fuc—	

No	Type	R1	R2
DFI: <i>m/z</i> 771.41; 591.35; 429.30			
36	D/E	Rha—Glc— Xyl	Glc—Glc—
37	D/E	Rha—Glc— Xyl	Glc—Glc—
38	D/E	Rha—Glc—	Glc—Glc—
40	D/E	Rha—Glc—	Glc—
41	D/E	Rha—Glc— Xyl	Glc—
42	D/E	Rha—Glc—	Glc—
43	D/E	Rha—Glc—	Glc—
DFI: <i>m/z</i> 755.42; 575.36; 413.31			
44	F	Rha—Glc— Xyl	Glc—Glc—
45	F	Rha—Glc— Xyl	Glc—Glc—
46	F	Rha—Glc—	Glc—Glc—
47	F	Rha—Glc—	Glc—Glc—
50	F	Acetyl—Rha—Glc— Xyl	Glc—Glc—
52	F	Rha—Glc— Xyl	Glc—
53	F	Rha—Glc—	Glc—
57	F	Acetyl—Rha—Glc— Xyl	Glc—
60	F	2Acetyl—Rha—Glc— Xyl	Glc—
61	F	2Acetyl—Rha—Glc— Xyl	Glc—

No	Type	R1	R2
DFI: <i>m/z</i> 753.40; 607.35; 445.30			
65	G	Rha—Glc—	
66	G	Rha—Glc— Xyl	
67	G	Rha—Glc—	
69	G	Acetyl—Rha—Glc— Xyl	
70	G	Acetyl—Rha—Glc— Xyl	
72	G	Acetyl—Rha—Glc—	
75	G	Acetyl—Rha—Glc—	
76	G	2Acetyl—Rha—Glc—	
Non-targets			
81	H	Xyl—Fuc— Rha	
49	I	Rha—Fuc— Glc	Glc—
55	I	Rha—Fuc— Xyl	Glc—
56	I	Rha—Fuc—	Glc—

Glc : β -D-Glucopyranosyl
 Rha : α -L-Rhamnopyranosyl
 Xyl : β -D-Xylopyranosyl
 Fuc : β -D-Fucopyranoside
 Ara : α -L-Arabinopyranosyl

* : ophiopogonin D was identified by the pure compound

Fig. 6. The identification of ophiopogonins based on diagnostic fragment ions strategy.

$[M-H-C_6H_{10}O_4-C_6H_{12}O_6]^-$. The characteristic loss of 180 Da from *m/z* 753.4012 to *m/z* 573.3340 indicated the conversion from furostanol to spirostanol glycosides. In addition, peak 49 and peak 55 were considered as the same type with the peak 56 since the same fragments were produced. The final identification was illustrated in Fig. 6.

Peak 64 gave the prominent MS^2 product ions at *m/z* 443.2776 ($C_{27}H_{39}O_5$) and 623.3416 ($C_{33}H_{51}O_{11}$), corresponding to $[M-H-C_6H_{10}O_4]^-$ and $[M-H-C_6H_{10}O_4-C_6H_{12}O_6]^-$. The representative loss of $C_6H_{12}O_6$ supported its assignment to spirostanol glycosides. Additionally, the predicted formula suggested that the aglycone might had an extra hydroxyl group, comparing with that of structure I (see Fig. 6) although we could not give the detail characterization. Peak 62 had the same fragmentation with the peak 64. Peak 58 exhibited predominant ions at *m/z* 557.3488, 737.4115, 883.4728, 1031.4931, and 1045.5297 in MS^2 spectrum. The mass difference between the *m/z* 557.3488 and 737.4115 was 180 Da, indicating the existence of glucose. Similar fragmentation pathway was observed for peak 59 and 54. However, for these compounds, too many database hits by single chemical formula querying constituted a great barrier to structural characterization. Therefore, they were considered as the tentative candidates of steroid saponin.

The left peaks including peaks 35, 39, 48, 51, 54 and 78 were also considered as the candidates of ophiopogonin since they could produce characteristic loss of sugar moiety. However, the structures could not be confirmed since no more sufficient supportive MS^n information was found.

3.3.3. The accuracy of MDF method

The accuracy of the MDF approach was calculated by the number of ophiopogonones/ophiopogonins identified by LCMS-IT-TOF dividing the number compounds screening by MDF. After filtering the components in *Ophiopogon japonicus* extract by the MDF, 34 compounds were distinguished which were in the mass defect ranges of ophiopogonones, and 62 compounds were distinguished which were in the mass defects ranges of ophiopogonins. Then the LCMS-IT-TOF was applied to characterize both targets and non-targets components in *Ophiopogon japonicus* extract for its MS^n function. The MS^n fragmentation patterns of 60 ophiopogonins and 29 ophiopogonones were then summarized, including 50 ophiopogonins and 27 ophiopogonones of detailed characterization. Based on the results of structural inference, the accuracy of the MDF method for ophiopogonins and ophiopogonones were 96.77% and 85.29%, respectively (see Table 3).

Table 3
Accuracy of the MDF approach applied in ophiopogonones and ophiopogonins.

	Ophiopogonones	Ophiopogonins
The MDF detection	34	62
Completely identified (targets ^b)	27 (20)	50 (46)
Potential compounds ^a	2	10
Accuracy (%)	85.29	96.77

^a The compounds present the obvious characteristic fragments or neutral loss information, indicating the potential candidates of ophiopogonones/ophiopogonins, although no final structural characterization was obtained because of the insufficient MSⁿ information.

^b The compounds structurally characterized according to the predefined fragments were considered as target compounds which can be easily detected by the conventional method. And other non-target compounds producing different fragments or insufficient MSⁿ information could only be detected by the MDF approach and then conducted further structural identification.

4. Conclusions

A primary challenge in herbal analysis was to enable global qualitative performance rapidly and accurately. In the present study, the MDF approach was developed and applied to rapidly identify the characteristic structural analogues from complex herbal extract. Compared with the conventional manual inspection and fragmentation-based method, the MDF approach enabled the original data to be analyzed much faster and more accurately by reducing the potential interferences of matrix ions. More importantly, this method can also be used for the rapid analysis of other homologous families in TCMs. However, it should be noted that the major limitation of this study was that only one authentic compound was used to validate the characterizing results, due to the authentic standards for most of the components identified being inaccessible.

Acknowledgments

This study was supported by National Nature Science Foundation (88102881, 30973583, and 30801422), the Project Program of State Key Laboratory of Natural Medicines, China Pharmaceutical University (No. JKGQ201109), the Program for New Century

Excellent Talents in University (NCET-09-0770), and a Foundation for the Author of National Excellent Doctoral Dissertation of PR China (Grant 200979).

Appendix A. Supplementary data

Supplementary data associated with this article can be found, in the online version, at doi:10.1016/j.chroma.2012.01.017.

References

- [1] R. Stone, *Science* 319 (2008) 709.
- [2] S.P. Boyle, P.J. Doolan, C.E. Andrews, R.G. Reid, *J. Pharm. Biomed. Anal.* 54 (2010) 951.
- [3] P. Li, L. Qi, E. Liu, J. Zhou, X. Wen, *Trends Anal. Chem.* 27 (2008) 66.
- [4] H. Zhang, Y. Wu, Y. Cheng, *J. Pharm. Biomed. Anal.* 31 (2003) 175.
- [5] X. Fan, W. Yi, Y. Cheng, *J. Pharm. Biomed. Anal.* 40 (2006) 591.
- [6] S. Li, S. Lai, J. Song, C. Qiao, X. Liu, Y. Zhou, H. Cai, B. Cai, H. Xu, *J. Pharm. Biomed. Anal.* 53 (2010) 946.
- [7] Y. Wang, Z. Guo, Y. Jin, X. Zhang, L. Wang, X. Xue, X. Liang, *J. Pharm. Biomed. Anal.* 51 (2010) 606.
- [8] G. Yan, H. Sun, W. Sun, L. Zhao, X. Meng, X. Wang, *J. Pharm. Biomed. Anal.* 53 (2010) 421.
- [9] G.L. Andrews, B.L. Simons, J.B. Young, A.M. Hawkridge, D.C. Muddiman, *Anal. Chem.* 83 (2011) 5442.
- [10] F. Song, Z. Liu, S. Liu, Z. Cai, *Anal. Chim. Acta* 531 (2005) 69.
- [11] L. Li, R. Tsao, J. Dou, F. Song, Z. Liu, S. Liu, *Anal. Chim. Acta* 536 (2005) 21.
- [12] J. Zhou, G. Xin, Z. Shi, M. Ren, L. Qi, H. Li, P. Li, *J. Chromatogr. A* 1217 (2010) 7109.
- [13] Y. Liang, H. Hao, A. Kang, L. Xie, T. Xie, X. Zheng, C. Dai, L. Wan, L. Sheng, G. Wang, *J. Chromatogr. A* 1217 (2010) 4971.
- [14] C. Zheng, H. Hao, X. Wang, X. Wu, G. Wang, G. Sang, Y. Liang, L. Xie, C. Xia, X. Yao, *J. Mass Spectrom.* 44 (2009) 230.
- [15] K.P. Bateman, J. Castro-Perez, M. Wrona, J.P. Shockcor, K. Yu, R. Oballa, D.A. Nicoll-Griffith, *Rapid Commun. Mass Spectrom.* 21 (2007) 1485.
- [16] M. Zhu, L. Ma, D. Zhang, K. Ray, W. Zhao, W.G. Humphreys, G. Skiles, M. Sanders, H. Zhang, *Drug Metab. Dispos.* 34 (2006) 1722.
- [17] H. Zhang, D. Zhang, K. Ray, M. Zhu, *J. Mass Spectrom.* 44 (2009) 999.
- [18] H. Hao, N. Cui, G. Wang, B. Xiang, Y. Liang, X. Xu, H. Zhang, J. Yang, C. Zheng, L. Wu, P. Gong, W. Wang, *Anal. Chem.* 80 (2008) 8187.
- [19] Y. Liang, H. Hao, L. Xie, A. Kang, T. Xie, X. Zheng, C. Dai, K. Hao, L. Sheng, G. Wang, *Drug. Metab. Dispos.* 38 (2010) 1747.
- [20] M. Ye, D. Guo, G. Ye, C. Huang, *J. Am. Soc. Mass Spectrom.* 16 (2005) 234.
- [21] Y. Lin, D. Zhu, J. Qi, M. Qin, B. Yu, *J. Pharm. Biomed. Anal.* 52 (2010) 757.
- [22] A. Perrone, T. Muzashvili, A. Napolitano, A. Skhirtladze, E. Kemertelidze, C. Pizza, S. Piacente, *Phytochemistry* 70 (2009) 2078.
- [23] T. Asano, T. Murayama, Y. Hirai, J. Shoji, *Chem. Pharm. Bull.* 41 (1993) 566.